

Upper bound on peak factor of N-multiple carriers

C. Tellambura

Indexing terms: Frequency division multiplexing, Modulation

An upper bound on the peak factor of an N carrier orthogonal frequency division multiplexing (OFDM) is derived. This bound highlights the intimate relationship between the peak factor and the out-of-phase aperiodic autocorrelation values of the data sequence.

Introduction: Multicarrier modulation techniques have been proposed for digital TV broadcasting and high speed wireless networks over multipath channels [1]. The principal drawback of multicarrier modulation is that the peak transmitted power may be up to N times the average, where N is the number of carriers. Linear amplifiers that can handle the peak power are inefficient. Hard limiting of the transmitted signal causes performance degradation and spectral sidelobe growth. Several solutions for overcoming this drawback have appeared in the literature following [2], which first described precoding of input sequences to reduce the peak factor. In this Letter an upper bound on the peak factor is derived. This bound highlights the intimate relationship between the peak factor and the out-of-phase aperiodic autocorrelation values of the data sequence.

Consider the periodic polynomial

$$P(t) = \sum_{n=1}^N a_n e^{in t} \quad (1)$$

where $i = \sqrt{-1}$, $|a_n| = 1$. If $\|P(t)\|_\infty = \max_t |P(t)|$, then the peak factor of $P(t)$ is defined as

$$\gamma = \frac{\|P(t)\|_\infty^2}{N} \quad (2)$$

If each a_n is allowed to take a finite number of discrete values, then finding a_1, a_2, \dots, a_N to minimise γ is a discrete optimisation problem, which has so far defied an analytical solution.

In engineering terms, $\|P(t)\|_\infty$ is just the peak envelope of a modulated carrier. Also, $\{a_n\}$ can be a binary or polyphase sequence. If a_n ($n = 1, \dots, N$) are modulated symbols (e.g. $a_n \in \{e^{2\pi i k l M} | k = 0, 1, \dots, M-1\}$ for M level phase shift keying), then $P(t)$ is the complex envelope of the modulated signal. The peak factor, γ , is useful for specifying the power capability of transmitters.

Theory:

Theorem: Let the aperiodic autocorrelation coefficients be

$$\rho(k) = \sum_{n=1}^{N-k} a_n a_{n+k}^* \quad \text{for } k = 0, \dots, N-1 \quad (3)$$

then the peak factor is bounded as

$$\gamma \leq 1 + \frac{2}{N} \sum_{k=1}^{N-1} |\rho(k)| \quad (4)$$

Proof of theorem:

$$|P(t)|^2 = \sum_{n=1}^N \sum_{k=1}^N a_k a_n^* e^{i(k-n)t} \quad (5a)$$

$$= N + 2\text{Re} \left\{ \sum_{n=1}^{N-1} \sum_{k=n+1}^N a_k a_n^* e^{i(k-n)t} \right\} \quad (5b)$$

$$= N + 2\text{Re} \left\{ \sum_{k=1}^{N-1} e^{ikt} \sum_{n=1}^{N-k} a_{n+k} a_n^* \right\} \quad (5c)$$

For any complex z , $\text{Re}(z) \leq |z|$ and $|\sum z_n| \leq \sum |z_n|$. Therefore, eqns. 2, 3 and 5c yield the upper bound in eqn. 4.

Eqn. 4 shows that binary or polyphase sequences with low out-of-phase aperiodic correlation values (i.e., small $\rho(k)$ for $k \geq 1$) can be used to construct low-peak-factor signals. Conversely, [3] notes that sequences that yield low-peak-factor signals also have low aperiodic autocorrelation. The problem of constructing sequences

with low aperiodic correlation has received much attention and has not been solved yet. It appears that the general problem of finding sequences that minimise the peak-factor is just as difficult.

Applications: The computation of γ is quite complex. Usually, kN samples (the integral $k \geq 1$) of $P(t)$ are computed by means of an FFT and the peak amplitude of these gives an estimate $\hat{\gamma}$ of γ . Clearly, $\hat{\gamma} \leq \gamma$. However, calculation of the upper bound in eqn. 4 is simpler.

Example 1: Consider (1, 1, 1, -1, 1) which is a Baker sequence. Its autocorrelation function is {5, 0, 1, 0, 1}. Hence applying eqn. 4 gives $\gamma \leq 1 + 4/5$; thus, the peak factor is < 2.55 dB. The peak factor in eqn. 2 is exactly 2.55dB. In this case, the upper bound coincides with the exact solution.

Example 2: Consider an 8-carrier OFDM system with each carrier being QPSK modulated. The difference in dB between eqns. 2 and 4 denoted by ϵ is plotted in Fig. 1 for all possible message sequences (2^6). For $\sim 84\%$ of message sequences, the upper bound is within a decibel of the exact solution.

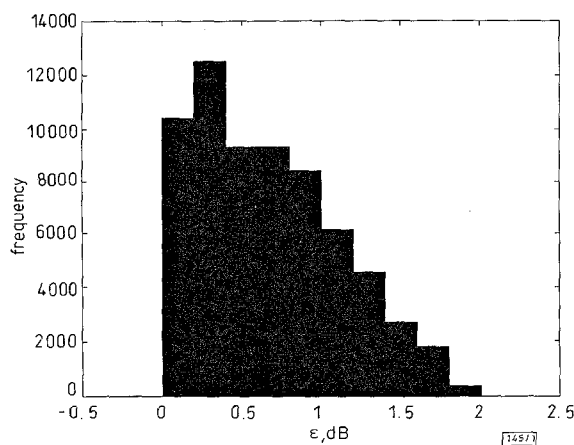


Fig. 1 Tightness of upper bound for 8-channel QPSK OFDM

Example 3: Consider the selective mapping (SLM) technique for reducing the peak factor [4] for a BPSK 16-carrier OFDM system. Let the information sequence be $p_0 = (m_0, m_1, \dots, m_{15})$ where $m_k \in \{1, -1\}$. Take the two complementary sequences $x_1 = (1, 1, 1, -1, 1, 1, -1, 1, 1, 1, -1, -1, -1, 1, -1)$ and $x_2 = (1, 1, 1, -1, 1, 1, -1, 1, 1, -1, -1, 1, 1, -1, 1)$. Define $p_k = p_0 \circ x_k$ where \circ denotes element-wise multiplication. Denote by $UB(p_k)$ the upper bound in eqn. 4 computed for p_k . If $UB(p_j) = \min\{UB(p_0), UB(p_1), UB(p_2)\}$, then p_j is selected for transmission. So this method needs an extra 1.58 bits ($\log_2 3$) to specify which p_j is transmitted. Fig. 2 shows the distribution of the peak factor for all possible message sequences. The maximum is about 8dB, which represents a 4dB reduction ($10 \log_{10} 16 = 12$ dB if no control is employed).

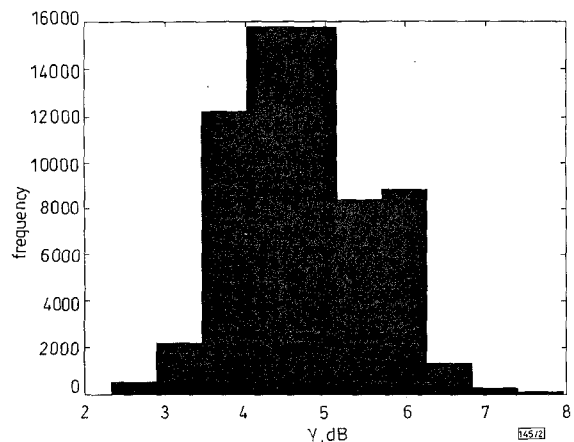


Fig. 2 Peak carrier distribution of a 16-carrier OFDM system with SLM

Example 4: Consider the simple peak factor reduction code derived here. Let the information sequence be $p_0 = (m_0, m_1, \dots, m_{n-1})$ where $m_k \in \{1, -1\}$. The encoder output is given by $p_e = (m_0, m_1, \dots, m_{n-1}, m_{n-2}, m_{n-3}, m_{n-4}, \dots)$. This encoding gives a rate $n/(2n-1)$ and length $N = 2n-1$ code. It can readily be shown that for k odd, $\rho(k)$ of p_e is zero. For example, when $n = 3$, $\rho(1) = \rho(3) = 0$ and $|\rho(2)| \leq 3$ and $|\rho(4)| = 1$. Thus our bound gives $\gamma \leq 2.6$, almost a 3dB reduction. For large N , the coding rate is almost 1/2. The sum of $|\rho(k)|$ for k even is bounded by $(N-1)^2/4$. Thus, the peak is bounded as $\gamma \leq 1 + (N-1)^2/(2N)$, a 3dB reduction.

Conclusions: A new upper bound for the peak factor of an N -carrier OFDM system has been derived. The bound only depends on the data sequence and may be useful for rapid elimination of sequences that have peak factors exceeding a given threshold.

© IEE 1997

Electronics Letters Online No: 19971069

19 June 1997

C. Tellambura (Department of Digital Systems, Monash University, Wellington Road, Clayton, Victoria 3168, Australia)

E-mail: chinhta@dgs.monash.edu.au

References

- 1 BINGHAM, J.A.C.: 'Multicarrier modulation for data transmission: an idea whose time has come', *IEEE Commun. Mag.*, 1990, pp. 5-14
- 2 JONES, A.E., WILKINSON, T.A., and BARTON, S.K.: 'Block coding scheme for reduction of peak to mean envelope power ratio of multicarrier transmission schemes', *Electron. Lett.*, 1994, **30**, pp. 2098-2099
- 3 SCHROEDER, M.R.: 'Synthesis of low-peak-factor signals and binary sequences with low autocorrelation', *IEEE Trans. Inform. Theory*, 1970, **IT-13**, pp. 85-89
- 4 BAUML, R.W., FISCHER, R.F.H., and HUBER, J.B.: 'Reducing the peak-to-average power ratio of multicarrier modulation by selected mapping', *Electron. Lett.*, 1996, **32**, pp. 2056-2057

Hybrid neural network/ray tracing model for radiowave penetration into buildings

J.W.H. Lee and A.K.Y. Lai

Indexing terms: Neural networks, Ray tracing

A feedforward multilayer neural network is used to predict the signal strength of building penetration. A ray tracing technique is employed to improve the prediction performance by introducing various separation distances and illustration angles into the modelling setup. The median prediction error is 1.69dB and the standard deviation is 1.15dB.

Introduction: As the usage pattern of personal communications moves indoors with the base station remaining outside, understanding of radiowave penetration into buildings becomes important. In the UHF band, ray tracing is widely used as a prediction tool for indoor and macrocell environments. Statistical analysis is another common method for radio planning.

Most recently, neural networks have been used in the development of radio propagation modelling [1, 2]. In this Letter, neural network and ray tracing techniques are combined to predict building penetration. Ray tracing is used to pinpoint the major scattering points in a non-LOS situation, the information derived is used in neural network modelling. We show that the additional parameters derived can improve the neural network modelling of building penetration.

Environment: In this Letter, we study the power penetration of the reading room in the Engineering building at the CUHK as shown in Fig. 1. The room size is $\sim 19\text{m} \times 19\text{m}$. The room has furniture such as a glass table, showcase and chair. A transmitter is placed on the roof of a building nearby, at least a 10m vertical distance above all the measurement points. The separation distance d_1 is

between 67.3 and 88.9m and the illustration angle a_1 varies between 10.5° and 26.7° . There is a metal-reinforced concrete bridge with extremely dense placement of metal ribs connecting the Engineering building and the building with the base station.

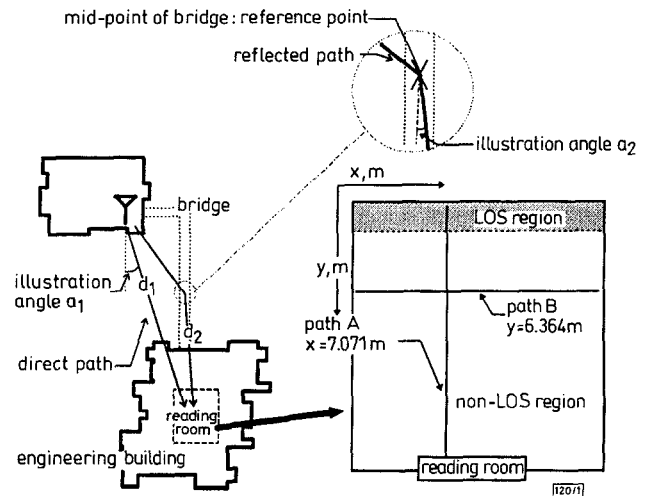


Fig. 1 Top view of measurement environment

d_2 is distance from mid-point of bridge to observation point

Problem formulation: The frequency of interest is 1.86GHz. A set of signal strengths at various sampling points is collected at three heights. The received power is measured as a function of the local co-ordinate, receiver height, illustration angle and separation distance from two reference points: the base station and the mid-point of the bridge. The base station is chosen for obvious reasons. The midpoint of the bridge is chosen because the bridge is a major scattering point redirecting signal into the reading room.

There were 642 pairs of data. Two subsets were formed. One subset containing 328 pairs was used as the training data for the neural network. The remaining 314 pairs were used to verify the performance of the trained neural network.

Eight models of the data were constructed as listed in Table 1.

Table 1: Difference in performance between the eight models

	Local co-ordinate	Receiver height	$\cos(a_1)$	$\log(d_1)$	$\cos(a_2)$	$\log(d_2)$	Mean error (dB)	Median error (dB)	Standard deviation (dB)	Maximum error (dB)
Model 1	×	×	-	-	-	-	2.001	1.792	1.237	11.75
Model 2	×	×	×	-	-	-	2.041	1.824	1.221	10.65
Model 3	×	×	-	×	-	-	2.015	1.824	1.259	12.18
Model 4	×	×	-	-	×	-	2.055	1.867	1.234	11.76
Model 5	×	×	-	-	-	×	1.946	1.737	1.123	6.117
Model 6	×	×	×	×	-	-	2.039	1.797	1.244	11.89
Model 7	×	×	-	-	×	×	1.997	1.824	1.088	5.832
Model 8	×	×	×	×	×	×	2.012	1.788	1.095	5.824

× used
- not used

The training data were not of the same composition for each model but there were an equal number. The whole set of data was presented to the neural network and the simulator used to calculate the prediction error of each data pair based on the rest of the data. 328 pairs with the least prediction error were then chosen to form the training data. For more information, refer to the filtration error in the AiNet Manual [3].

Results: We used a neural network simulation program called AiNet [3]. From the statistical information, model 5 has the least mean and median error while models 7 and 8 have the least maximum error with reasonably low median and mean error. We can conclude that models 5, 7 and 8 are the best for modelling the problem. Fig. 2 compares the predicted and measured values